IEEE Access
Multidisciplinary | Rapid Review | Open Access Journal

Received November 24, 2018, accepted December 6, 2018, date of publication December 11, 2018,
date of current version January 7, 2019.

Digital Object Identifier 10.1109/ACCESS.2018.2886248

Beamforming and Resource Allocation for a Multi-Pair Wireless Powered Two-Way Relay Network With Fairness

GERARDO SACARELO[1], IICKHO SONG[2], AND YUN HEE KIM[1]
[1]Department of Electronic Engineering, Kyung Hee University, Yongin 17104, South Korea
[2]School of Electrical Engineering, Korea Advanced Institute of Science and Technology, Daejeon 34141, South Korea

Corresponding author: Yun Hee Kim (yheekim@khu.ac.kr)

This work was supported by the National Research Foundation of Korea (NRF) through the Korean Government under Grant NRF-2018R1D1A1B07045515 and Grant NRF-2018R1A2A1A05023192.

ABSTRACT We consider a wireless powered two-way relay network in which a multi-antenna relay transfers power to devices and assists multi-pair data exchanges based on decode-and-forward with network coding in three phases. The relay in the network adopts energy beamforming (BF) for wireless power transfer, zero-forcing receive BF for multiple access decoding, and two-step transmit BF for efficient transmission of the network coded symbols by eliminating inter-pair interference. In this setup, we optimize energy the BF and transmit BF as well as the time allocation in order to maximize the rate fairness among the devices. The optimal energy BF is derived in closed-form for the network with two devices and is found by searching through the span of channel matched filters with more than two devices, while the optimal two-step transmit BF is given in closed-form for an arbitrary number of devices. In addition, the time allocation problem is shown to be convex and thus easily solved with the existing convex optimization solvers. The simulation results show that the proposed network outperforms conventional networks significantly due to the enhanced BF and flexible time allocation methods.

INDEX TERMS Beamforming, decode-and-forward, max-min fairness, two-way relay, wireless powered communication.

I. INTRODUCTION

Recently, remote wireless power transfer (WPT) has been implemented into wireless communications to overcome the limitations of battery size and deployment areas, which are encountered when developing many Internet of things (IoT) applications [1]–[8]. By harvesting energy from the radio frequency signal, WPT enables battery-limited devices to be sustainable without frequent battery replacements or even without batteries. There exist two basic ways of introducing WPT into wireless information transfer (WIT): simultaneous wireless information and power transfer (SWIPT) and wireless powered communication networking (WPCN). In SWIPT, generally incorporated in the downlink, power and data flows are in the same direction [1], [2], [8]. In contrast, WPCN, which is of our main concern, provides power and data flows in different directions, e.g., WPT in the downlink and WIT in the uplink [3]–[7].

Initial studies on WPCN were devoted to data collection from multiple battery-limited devices, where a hybrid access point (HAP) transmits power to the devices in the downlink WPT and the devices transfer data using the harvested energy in the uplink WIT [3], [9]–[17]; this protocol will be called the wireless powered multiple access (WP-MAC) for the simplicity in the sequel. For WP-MAC, the uplink WIT was generally supported either in time division multiple access (TDMA) with a single-antenna HAP or in space division multiple access (SDMA) with a multi-antenna HAP. The sum rate of the uplink WIT in TDMA was optimized via time allocation [3], [15], [16] and power and time allocation [11], [14] to the WPT and WIT TDMA slots. When a multi-antenna HAP was employed in WP-MAC to support the uplink WIT in SDMA, not only power and time allocation but also beamforming (BF) optimization for WPT and for WIT was performed for maximum throughput or maximum fairness [9], [10], [12], [13], [17]. These studies showed the benefits of multiple antenna BF schemes to both WPT and WIT by focusing the energy on the desired devices while reducing the interferences among the devices in WIT.

Recently, WPCN was built with more complicated but spectrally efficient two-way relay (TWR) protocols [18]–[29], in which the communication devices exchange their data with the help of a relay in two phases to extend their communication ranges; the devices simultaneously transmit data to the relay in the multiple access (MAC) phase like the uplink WIT in WP-MAC, and the relay sends the MAC signal to the devices via amplify-and-forward (AF) or decode-and-forward (DF) in the broadcasting (BC) phase. The WPCN for TWR was designed for a device to charge a relay by introducing SWIPT in the MAC phase [18]–[21], [24]–[26]. For a relay to charge the devices, the WPCN for TWR was designed by adding the WPT phase or by introducing SWIPT in the BC phase [22], [23], [27]–[29].

In this paper, we address a wireless powered (WP)-TWR network, in which a multi-antenna relay charges the devices and supports the data exchange among the devices in SDMA through BF and resource allocation.

A. RELATED WORK

Since WP-MAC resembles the WP-TWR with an additional WPT phase in some aspects, we first introduce the BF design and resource allocation problems tackled for WP-MAC. For single-antenna devices, the energy BF for WPT, receive BF for WIT, and time allocation to the WPT and WIT phases were optimized in order to maximize the minimum rate toward the fairness [9], where optimal BF solutions were found via an iterative algorithm. The WP-MAC with a massive-antenna HAP and single-antenna devices was analyzed by including an uplink channel estimation phase and an asymptotically optimal solution was found in the sense of maximizing the minimum rate with respect to power and time allocation [10]. The sum rate, instead of the minimum rate in [9], was maximized by optimizing energy BF and receive BF iteratively for the given time allocation and then optimizing the time allocation in [12]. The BF and resource allocation problems were also studied with multi-antenna devices to maximize the sum rate [13] and to maximize the minimum rate [17] by solving dual problems. However, to solve the dual problems, BF optimization is required whenever the time allocation changes.

For the WP-TWR network, BF and resource allocation methods were studied with diverse relaying strategies, yet in different directions depending on the assumption on the energy state of the devices. For devices with enough energy for MAC transmission, two-phase WP-TWR protocols were designed with SWIPT in the BC phase [23], [27]–[29], where a device employs a power splitting (PS) receiver for simultaneous energy harvesting and information decoding. The PS ratios were optimized jointly with HAP transmit BF to minimize the total transmit power under the rate constraints for DF WP-TWR [23], to maximize the weighted sum energy of two devices for both AF WP-TWR and DF WP-TWR [27], and to maximize the energy efficiency of AF WP-TWR [28]. In [29], only the PS ratios were optimized to maximize the sum rate of DF WP-TWR when a massive-antenna HAP employs zero forcing (ZF) or matched filter (MF) for receive BF, and MF for transmit BF. It should be noted that all these studies assumed equal time allocation for the MAC and BC phases although DF allows unequal time allocation to the MAC and BC phases. On the other hand, for the devices having insufficient energy for MAC transmission, [22] designed three-phase AF WP-TWR with WPT, MAC, and BC phases by employing the energy BF of [10] for WPT and the ZF-based joint receive/transmit BF [30] for AF TWR, where the spectral and energy efficiencies were analyzed without any optimization. To the best of our knowledge, BF and resource allocation problems have not yet been studied for the three-phase WP-TWR protocol.

B. MOTIVATION AND CONTRIBUTIONS

As elaborated in the related work section, most studies on WP-TWR are based on SWIPT in the BC phase, additionally assuming that the devices have the necessary energy for MAC transmission. However, the battery-limited devices in an initial data exchange or in a sporadic data exchange may have no energy for MAC transmission; in this case, the WPT phase should precede the MAC phase so the devices can harvest the energy before data transmission. However, these three-phase WP-TWR protocols were studied with AF only in [22], which might not be suitable for the WP-TWR suffering from a doubly near-far problem in the MAC; the AF suffers from noise amplification when amplifying a weak MAC signal and a large performance mismatch in the MAC and BC phases due to the equal time allocation required for the AF.

This paper designs a three-phase WP-TWR protocol by employing DF with network coding [25] to support multi-pair TWR more efficiently. Unlike AF WP-TWR in [22], DF WP-TWR enables flexible time allocation into the three phases that balances a mismatch in the MAC and BC performances, and allows flexible BF designs such that the design of transmit BF in the BC phase is independent of that of energy BF and receive BF. In addition, DF with network coding improves the performance of the BC phase by reducing the number of spatially multiplexed symbols. We consider practically implementable modular BF schemes such as multicast energy BF for WPT, ZF-based receive BF for the MAC, and two-step transmit BF eliminating the inter-pair interference [31] for the BC. In this setup, we solve the problem of maximizing the minimum rate of the devices by optimizing energy BF, transmit BF, and time allocation, which has not been studied for WP-TWR.

The main contributions of this paper are summarized as follows:

- We propose a multi-pair DF WP-TWR protocol exploiting three phases of unequal time durations. For this protocol, we propose two-step BF consisting of inter-pair interference nulling BF and pairwise BF with power allocation; this enables efficient transmission of the network coding to the desired pair without intervention with the other pairs in the BC phase.

- We formulate the problem of optimizing energy BF, transmit BF, and time allocation to maximize the minimum rate of the devices in WP-TWR for maximum fairness. This max-min rate optimization problem for WP-TWR is different from those for WP-MAC [9], [10], [17], in that the former has additional transmit BF optimization for the BC and time allocation over three phases instead of only two phases as in the latter.
- The problem is transformed into an equivalent problem consisting of three subproblems: energy BF optimization and transmit BF optimization problems that maximize the minimum signal-to-noise power ratio (SNR) in the MAC and BC phases, respectively, and the subsequent time allocation problem to maximize the minimum rate. The two BF problems are independent of time allocation and are solved only once, unlike the problems for WP-MAC [9], [17] which should be solved for each given time allocation. The time-independent BF problems are more favorable in WP-TWR, which performs time allocation over three phases.
- We prove that the optimal energy BF is given as a linear combination of the channel matched vectors with complex-valued weights. The optimal energy BF is derived in closed-form for a single device pair, and is found for multiple device pairs by searching complex-valued weights via existing algorithms developed for the multicast BF [32]–[36] at a reduced complexity. The proposed energy BF is shown to outperform conventional energy BF, given as a linear combination of the channel matched vectors with real-valued weights [10], [22].
- The optimal solution for the transmit BF is provided in closed-form by deriving the optimal pairwise BF and inter-pair power allocation explicitly for two-step transmit BF.
- The time allocation problem is shown to be convex and so can be solved with existing convex optimization solvers. The benefit of the time allocation is shown in the performance evaluation.

The remainder of this paper is organized as follows: Section II describes the system model of the WP-TWR network with multiple device pairs and formulates the max-min rate optimization problem. Section III tackles the problem by optimizing BF methods for the given time allocation and then optimizing the time allocation. The performance of the proposed network is investigated by varying the BF and time allocation methods in Section IV. Finally, concluding remarks are provided in Section V.

Notation: We use $(\cdot)^*$, $(\cdot)^T$, and $(\cdot)^H$ for the conjugate, transpose, and Hermitian transpose of a vector or a matrix, respectively, and $r(\cdot)$, $(\cdot)^{1/2}$, $\mathrm{tr}(\cdot)$, and $\det(\cdot)$ for the rank, square-root, trace, and determinant of a matrix, respectively. In addition, $\mathrm{diag}(\boldsymbol{a})$ is the diagonal matrix with vector $\boldsymbol{a}$ on the diagonal and $[\boldsymbol{A}]_{k,l}$ denotes the (k,l)-th element of a matrix $\boldsymbol{A}$. We use $\mathbf{0}_n$ to represent the length-n vector with all zero entries and $\boldsymbol{I}_n$ to represent the $n \times n$ identity matrix.

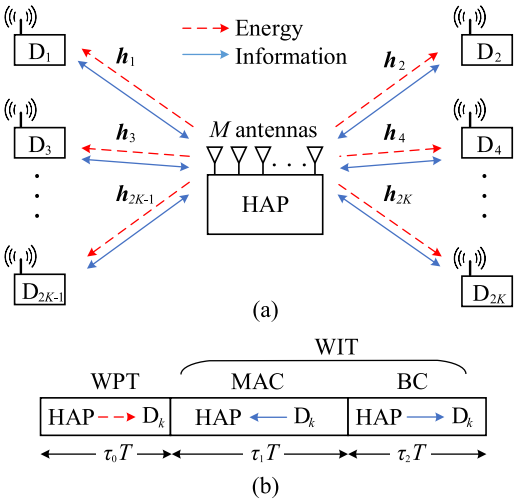

FIGURE 1. WP-TWR network: (a) system model, (b) protocol.

The set of length-n vectors is denoted by $\mathbb{R}_+^n$ for non-negative real entries and $\mathbb{C}^n$ for complex entries, while the set of $n \times m$ complex matrices is denoted by $\mathbb{C}^{n\times m}$. For random variables, $\sim$ signifies 'distributed as' and $\mathsf{CN}(\boldsymbol{\mu}, \boldsymbol{\Sigma})$ denotes the distribution of a complex Gaussian random vector with mean $\boldsymbol{\mu}$ and covariance matrix $\boldsymbol{\Sigma}$.

II. SYSTEM MODEL AND PROBLEM FORMULATION

A. SYSTEM MODEL

Consider a WP-TWR network consisting of a single relay, called HAP, and $2K$ devices $\{\mathrm{D}_k\}_{k=1}^{2K}$, as seen in Fig. 1(a). The HAP equipped with M antennas is capable of power and information transfer. Each device equipped with a single antenna is capable of energy harvesting and information transfer. Under the assumption of channel reciprocity and flat Rayleigh fading, the channels between the HAP and the devices are described by the $M \times 2K$ matrix

$$\boldsymbol{H} = [\boldsymbol{h}_1, \boldsymbol{h}_2, \cdots, \boldsymbol{h}_{2K}], \tag{1}$$

where $\boldsymbol{h}_k \sim \mathsf{CN}(\mathbf{0}_M, \omega_k \boldsymbol{I}_M)$ denotes the channel vector between the HAP and D_k subject to path loss ω_k. The channels between the devices are uncorrelated each other.

In the network, devices D_{2p-1} and D_{2p} form a communication pair for $p = 1, 2, \cdots, K$. The HAP not only transfers the power to the devices, but also assists their data exchanges via the DF-based WP-TWR protocol depicted in Fig. 1(b). The protocol consists of the WPT, MAC, and BC phases of durations $\tau_0 T$, $\tau_1 T$, and $\tau_2 T$, respectively, where $\tau_i > 0$ for $i = 0, 1, 2$ and $\sum_{i=0}^{2} \tau_i = 1$; here, $T = 1$ is assumed without a loss of generality. The HAP transfers wireless power to the devices in the WPT phase. By consuming the energy harvested in the WPT phase, the devices simultaneously transmit the symbols containing the messages to the HAP. In the BC phase, the HAP broadcasts the network coding of the decoded messages in the MAC phases to the devices, and the devices decode the network coded symbols from the received signals to retrieve the messages sent by their partners. Unlike the AF WP-TWR protocol [22], the proposed DF WP-TWR

protocol allows unequal time allocation for the MAC and BC phases, as $\tau_1 \neq \tau_2$ due to the regenerative relay signal.

In the WPT phase, the HAP transfers the power P_H with the energy BF $\boldsymbol{w}$ subject to $\|\boldsymbol{w}\|^2 = 1$. The energy harvested at D_k can be written as

$$E_k = \tau_0 \eta \mathsf{P}_\mathrm{H} \left| \boldsymbol{h}_k^T \boldsymbol{w} \right|^2, \tag{2}$$

where η is the energy harvesting efficiency and the noises are ignored. In the MAC phase, device D_k transmits symbol x_k containing message m_k to the HAP with transmit power

$$P_k = \frac{E_k}{\tau_1} = \eta \mathsf{P}_\mathrm{H} \left| \boldsymbol{h}_k^T \boldsymbol{w} \right|^2 \frac{\tau_0}{\tau_1} \tag{3}$$

by consuming all the harvested energy (2).

The signal received at the HAP in the MAC phase is then expressed as

$$\boldsymbol{y}_1 = \boldsymbol{H} \boldsymbol{P}_\mathrm{D}^{1/2} \boldsymbol{x} + \boldsymbol{n}_1, \tag{4}$$

where $\boldsymbol{x} = [x_1, x_2, \cdots, x_{2K}]^T \sim \mathsf{CN}(\boldsymbol{0}_{2K}, \boldsymbol{I}_{2K})$ is the symbol vector, $\boldsymbol{P}_\mathrm{D} = \mathrm{diag}([P_1, P_2, \cdots, P_{2K}]^T)$ is the transmit power matrix, and $\boldsymbol{n}_1 \sim \mathsf{CN}(\boldsymbol{0}_M, \sigma_1^2 \boldsymbol{I}_M)$ is the noise vector at the HAP. The HAP applies the $2K \times M$ ZF receive BF matrix $\boldsymbol{\Phi}_1^H = \left(\boldsymbol{H}^H \boldsymbol{H}\right)^{-1} \boldsymbol{H}^H$ of complexity $O(M(2K)^2 + (2K)^3)$ [37] to (4) as

$$z_1 = \boldsymbol{\Phi}_1^H \boldsymbol{y}_1 = \boldsymbol{P}_\mathrm{D}^{1/2} \boldsymbol{x} + \boldsymbol{\Phi}_1^H \boldsymbol{n}_1 \tag{5}$$

from which the message $\hat{m}_k$ contained in x_k is decoded for $k = 1, 2, \cdots, 2K$. The HAP then constructs the network coded symbol $x_{\mathrm{bc},p}$ of decoded messages $\hat{m}_{2p-1}$ and $\hat{m}_{2p}$ for each communication pair $p \in \{1, 2, \cdots, K\}$.

In the BC phase, the HAP transmits the symbol vector $\boldsymbol{x}_\mathrm{bc} = [x_{\mathrm{bc},1}, x_{\mathrm{bc},2}, \cdots, x_{\mathrm{bc},K}]^T$ to the devices with $M \times K$ transmit BF matrix $\boldsymbol{\Phi}_2$ subject to $\mathrm{tr}(\boldsymbol{\Phi}_2 \boldsymbol{\Phi}_2^H) = 1$. The received signal $y_{2,k}$ at device D_k is arranged in vector $\boldsymbol{y}_2 = [y_{2,1}, y_{2,2}, \cdots, y_{2,2K}]^T$ given by

$$\boldsymbol{y}_2 = \sqrt{\mathsf{P}_\mathrm{H}} \boldsymbol{H}^T \boldsymbol{\Phi}_2 \boldsymbol{x}_\mathrm{bc} + \boldsymbol{n}_2, \tag{6}$$

where $\boldsymbol{n}_2 \sim \mathsf{CN}(\boldsymbol{0}_{2K}, \sigma_2^2 \boldsymbol{I}_{2K})$ is the vector of the noises at the devices.

We adopt two-step transmit BF, which steers the K beams to K device pairs with appropriate power allocation while avoiding the inter-pair interference. Specifically, the transmit BF is given by

$$\boldsymbol{\Phi}_2 = \left[\tilde{\boldsymbol{V}}_1^{(0)} \boldsymbol{b}_1, \tilde{\boldsymbol{V}}_2^{(0)} \boldsymbol{b}_2, \cdots, \tilde{\boldsymbol{V}}_K^{(0)} \boldsymbol{b}_K \right], \tag{7}$$

where $\tilde{\boldsymbol{V}}_p^{(0)} \in \mathbb{C}^{M \times L}$ is formed by the basis vectors of the null space of the channel $\tilde{\boldsymbol{H}}_p^T = \left[\boldsymbol{h}_1, \cdots, \boldsymbol{h}_{2p-2}, \boldsymbol{h}_{2p+1}, \cdots, \boldsymbol{h}_{2K} \right]^T$ excluding the pth pair and $\boldsymbol{b}_p \in \mathbb{C}^L$ is the pairwise BF vector directed to the p-th pair for $L \geq M - 2K + 2$.

Here, we obtain $\tilde{\boldsymbol{V}}_p^{(0)}$ by taking the submatrix of $\tilde{\boldsymbol{V}}_p$ corresponding to zero singular values from singular value decomposition $\tilde{\boldsymbol{H}}_p^T = \tilde{\boldsymbol{U}}_p \tilde{\boldsymbol{\Sigma}}_p \tilde{\boldsymbol{V}}_p^H$. The pairwise BF is subject to

$$\sum_{p=1}^{K} \|\boldsymbol{b}_p\|^2 = 1 \tag{8}$$

to obtain the transmit power P_H from $\mathrm{tr}(\boldsymbol{\Phi}_2 \boldsymbol{\Phi}_2^H) = \sum_{p=1}^{K} \boldsymbol{b}_p^H (\tilde{\boldsymbol{V}}_p^{(0)})^H \tilde{\boldsymbol{V}}_p^{(0)} \boldsymbol{b}_p = 1$.

With the proposed transmit BF, the received signal at device D_k is described by

$$y_{2,k} = \sqrt{\mathsf{P}_\mathrm{H}} \boldsymbol{g}_k^T \boldsymbol{b}_{\lceil k/2 \rceil} x_{\mathrm{bc},\lceil k/2 \rceil} + n_{2,k}, \tag{9}$$

where $\lceil \cdot \rceil$ is the ceiling operation and $\boldsymbol{g}_k = (\tilde{\boldsymbol{V}}_{\lceil k/2 \rceil}^{(0)})^T \boldsymbol{h}_k$ is the effective channel after applying the first-step BF nulling the inter-pair interference. It is clear that there is no inter-pair interference at a device in receiving the network coded symbol $x_{\mathrm{bc},p}$ common to its partner.

B. PROBLEM FORMULATION

This section formulates the problem of maximizing the minimum rate of $2K$ data flows in the network toward the maximum fairness. For this purpose, we first obtain the achievable rate in transferring the message m_k from D_k to $\mathrm{D}_{p(k)}$ for $k = 1, 2, \cdots, 2K$, where $p(k) = k + 1$ for odd k and $p(k) = k - 1$ for even k. The achievable rate from D_k to $\mathrm{D}_{p(k)}$ is given by

$$\mathsf{R}_k = \min(\mathsf{R}_{1,k}, \mathsf{R}_{2,p(k)}) \text{ bps/Hz}, \tag{10}$$

where $\mathsf{R}_{1,k}$ is the achievable rate from D_k to the HAP in the MAC phase and $\mathsf{R}_{2,k}$ is the achievable rate from the HAP to D_k in the BC phase. The rate of each phase is given by

$$\mathsf{R}_{i,k} = \tau_i \log_2(1 + \gamma_{i,k}), \quad i = 1, 2, \tag{11}$$

where $\gamma_{1,k}$ and $\gamma_{2,k}$ are the instantaneous SNR of (5) and (9), respectively, derived as

$$\gamma_{1,k} = \frac{P_k}{\sigma_1^2 \left[\boldsymbol{\Phi}_1^H \boldsymbol{\Phi}_1 \right]_{k,k}} = \eta \frac{\tau_0}{\tau_1} \frac{\mathsf{P}_\mathrm{H}}{\sigma_1^2} \beta_k^2 |\boldsymbol{h}_k^T \boldsymbol{w}|^2 \tag{12}$$

and

$$\gamma_{2,k} = \frac{\mathsf{P}_\mathrm{H}}{\sigma_2^2} |\boldsymbol{g}_k^T \boldsymbol{b}_{\lceil k/2 \rceil}|^2, \tag{13}$$

with $1/\beta_k^2 = \left[\boldsymbol{\Phi}_1^H \boldsymbol{\Phi}_1 \right]_{k,k} = \left[(\boldsymbol{H}^H \boldsymbol{H})^{-1} \right]_{k,k}$.

We maximize the minimum rate in the network by optimizing the energy BF vector $\boldsymbol{w}$, the pairwise BF vectors $\boldsymbol{B} = [\boldsymbol{b}_1, \boldsymbol{b}_2, \cdots, \boldsymbol{b}_K]$, and the time allocation vector $\boldsymbol{\tau} = [\tau_0, \tau_1, \tau_2]^T$.

The max-min rate optimization problem is then formulated as

$$\max_{\boldsymbol{w}, \boldsymbol{B}, \boldsymbol{\tau}} \ \mathsf{R}_\mathrm{min}(\boldsymbol{w}, \boldsymbol{B}, \boldsymbol{\tau}) \tag{14a}$$

$$\text{s.t. } \boldsymbol{w} \in \mathcal{C}_{\boldsymbol{w}}, \ \boldsymbol{B} \in \mathcal{C}_{\boldsymbol{B}}, \ \boldsymbol{\tau} \in \mathcal{C}_{\boldsymbol{\tau}}, \tag{14b}$$

where the constraint sets are defined as $\mathcal{C}_{\boldsymbol{w}} = \{\boldsymbol{w} | \boldsymbol{w} \in \mathbb{C}^M, \|\boldsymbol{w}\|^2 = 1\}$, $\mathcal{C}_{\boldsymbol{B}} = \{\boldsymbol{B} | \boldsymbol{B} \in \mathbb{C}^{L \times K}, \mathrm{tr}(\boldsymbol{B}^H \boldsymbol{B}) = 1\}$, and $\mathcal{C}_{\boldsymbol{\tau}} = \{\boldsymbol{\tau} | \boldsymbol{\tau} \in \mathbb{R}_+^3, \sum_{i=0}^{2} \tau_i = 1\}$. The objective function is written as

$$\mathsf{R}_\mathrm{min}(\boldsymbol{w}, \boldsymbol{B}, \boldsymbol{\tau}) = \min_{1 \leq k \leq 2K} \min\{\mathsf{R}_{1,k}(\boldsymbol{w}, \boldsymbol{\tau}), \mathsf{R}_{2,p(k)}(\boldsymbol{B}, \boldsymbol{\tau})\} \tag{15}$$

from (10) after including the arguments of $\mathsf{R}_{i,k}$ to show their dependency explicitly. From the associative property of the minimum operation, (15) is also rewritten as

$$\mathsf{R}_{\min}(\boldsymbol{w}, \boldsymbol{B}, \boldsymbol{\tau}) = \min\left\{\mathsf{R}_{1,\min}(\boldsymbol{w}, \boldsymbol{\tau}), \mathsf{R}_{2,\min}(\boldsymbol{B}, \boldsymbol{\tau})\right\}, \quad (16)$$

where

$$\mathsf{R}_{1,\min}(\boldsymbol{w}, \boldsymbol{\tau}) = \min_{1\le k\le 2K} \mathsf{R}_{1,k}(\boldsymbol{w}, \boldsymbol{\tau}) \quad (17)$$

and

$$\mathsf{R}_{2,\min}(\boldsymbol{B}, \boldsymbol{\tau}) = \min_{1\le k\le 2K} \mathsf{R}_{2,k}(\boldsymbol{B}, \boldsymbol{\tau}). \quad (18)$$

III. OPTIMIZATION OF BF AND TIME ALLOCATION

We now transform problem (14) into three equivalent subproblems by exploiting a general principle of optimization via exhaustive searching that we can always optimize a function by first optimizing over some of the variables while fixing the other variables, and then optimizing over the remaining variables [38]. Since the constraint sets $\mathcal{C}_{\boldsymbol{w}}$, $\mathcal{C}_{\boldsymbol{B}}$, and $\mathcal{C}_{\boldsymbol{\tau}}$ in (14) are independent of each other, the subproblems searching the solution to (14) over $(\boldsymbol{w}, \boldsymbol{B}, \boldsymbol{\tau}) \in \mathcal{C}_{\boldsymbol{w}} \times \mathcal{C}_{\boldsymbol{B}} \times \mathcal{C}_{\boldsymbol{\tau}}$ can be expressed in simpler forms as follows.

By fixing $\boldsymbol{B}$ and $\boldsymbol{\tau}$, we first solve

$$\max_{\boldsymbol{w}\in\mathcal{C}_{\boldsymbol{w}}} \mathsf{R}_{\min}(\boldsymbol{w}, \boldsymbol{B}, \boldsymbol{\tau}) \quad (19)$$

to find the optimal solution $\boldsymbol{w}^{\dagger}(\boldsymbol{B}, \boldsymbol{\tau})$ and optimal value $\tilde{\mathsf{R}}_{\min}(\boldsymbol{B}, \boldsymbol{\tau}) = \mathsf{R}_{\min}(\boldsymbol{w}^{\dagger}(\boldsymbol{B}, \boldsymbol{\tau}), \boldsymbol{B}, \boldsymbol{\tau})$ for each $(\boldsymbol{B}, \boldsymbol{\tau}) \in \mathcal{C}_{\boldsymbol{B}} \times \mathcal{C}_{\boldsymbol{\tau}}$. Next, by fixing $\boldsymbol{\tau}$, we solve

$$\max_{\boldsymbol{B}\in\mathcal{C}_{\boldsymbol{B}}} \tilde{\mathsf{R}}_{\min}(\boldsymbol{B}, \boldsymbol{\tau}) \quad (20)$$

to obtain the optimal solution $\boldsymbol{B}^{\dagger}(\boldsymbol{\tau})$ and optimal value $\tilde{\tilde{\mathsf{R}}}_{\min}(\boldsymbol{\tau}) = \tilde{\mathsf{R}}_{\min}(\boldsymbol{B}^{\dagger}(\boldsymbol{\tau}), \boldsymbol{\tau})$ for each $\boldsymbol{\tau} \in \mathcal{C}_{\boldsymbol{\tau}}$. Finally, we solve

$$\max_{\boldsymbol{\tau}\in\mathcal{C}_{\boldsymbol{\tau}}} \tilde{\tilde{\mathsf{R}}}_{\min}(\boldsymbol{\tau}) \quad (21)$$

to obtain the optimal solution $\boldsymbol{\tau}^{\dagger}$. From the solutions of (19)-(21), the optimal solution $(\boldsymbol{w}^o, \boldsymbol{B}^o, \boldsymbol{\tau}^o)$ to (14) is obtained as $\boldsymbol{w}^o = \boldsymbol{w}^{\dagger}(\boldsymbol{B}^{\dagger}(\boldsymbol{\tau}^{\dagger}), \boldsymbol{\tau}^{\dagger})$, $\boldsymbol{B}^o = \boldsymbol{B}^{\dagger}(\boldsymbol{\tau}^{\dagger})$, and $\boldsymbol{\tau}^o = \boldsymbol{\tau}^{\dagger}$. Since only $\mathsf{R}_{1,\min}$, but not $\mathsf{R}_{2,\min}$, depends on $\boldsymbol{w}$ in (16) and the constraints sets $\mathcal{C}_{\boldsymbol{w}}$, $\mathcal{C}_{\boldsymbol{B}}$, and $\mathcal{C}_{\boldsymbol{\tau}}$ are independent, the solution to (19) can be found by solving

$$\max_{\boldsymbol{w}\in\mathcal{C}_{\boldsymbol{w}}} \mathsf{R}_{1,\min}(\boldsymbol{w}, \boldsymbol{\tau}) \quad (22)$$

for each $\boldsymbol{\tau} \in \mathcal{C}_{\boldsymbol{\tau}}$. The solution to (22) is also obtained by solving

$$\max_{\boldsymbol{w}\in\mathcal{C}_{\boldsymbol{w}}} \left\{\min_{1\le k\le 2K} \gamma_{1,k}\right\}, \quad (23)$$

or equivalently,

$$\max_{\boldsymbol{w}\in\mathcal{C}_{\boldsymbol{w}}} \left\{\min_{1\le k\le 2K} \beta_k^2 |\boldsymbol{h}_k^T \boldsymbol{w}|^2\right\} \quad (24)$$

since $\mathsf{R}_{1,k}(\boldsymbol{w}, \boldsymbol{\tau}) = \tau_1 \log_2\left(1 + \gamma_{1,k}\right)$ is a monotonically increasing function of $\gamma_{1,k} = \eta \frac{\tau_0}{\tau_1} \frac{\mathsf{P}_{\mathrm{H}}}{\sigma_1^2} \beta_k^2 |\boldsymbol{h}_k^T \boldsymbol{w}|^2$ for fixed $\boldsymbol{\tau}$.

The objective function and the constraint set in (24) do not depend on $\boldsymbol{B}$ and $\boldsymbol{\tau}$ so that we have $\boldsymbol{w}^{\dagger}(\boldsymbol{B}, \boldsymbol{\tau}) = \boldsymbol{w}^{\dagger}$ for all $(\boldsymbol{B}, \boldsymbol{\tau}) \in \mathcal{C}_{\boldsymbol{B}} \times \mathcal{C}_{\boldsymbol{\tau}}$. Therefore, the optimal energy BF for problem (14) is obtained as $\boldsymbol{w}^o = \boldsymbol{w}^{\dagger}$.

Similarly, the solution $\boldsymbol{B}^{\dagger}(\boldsymbol{\tau})$ to (20) is obtained by solving

$$\max_{\boldsymbol{B}\in\mathcal{C}_{\boldsymbol{B}}} \mathsf{R}_{2,\min}(\boldsymbol{B}, \boldsymbol{\tau}) \quad (25)$$

for each $\boldsymbol{\tau} \in \mathcal{C}_{\boldsymbol{\tau}}$ since $\tilde{\mathsf{R}}_{\min}(\boldsymbol{B}, \boldsymbol{\tau}) = \min\{\mathsf{R}_{1,\min}(\boldsymbol{w}^{\dagger}, \boldsymbol{\tau}), \mathsf{R}_{2,\min}(\boldsymbol{B}, \boldsymbol{\tau})\}$. Again, (25) is equivalent to

$$\max_{\boldsymbol{B}\in\mathcal{C}_{\boldsymbol{B}}} \left\{\min_{1\le k\le 2K} \gamma_{2,k}\right\} \quad (26)$$

for the same reason as that applied to the energy BF optimization. The solution $\boldsymbol{B}^{\dagger}(\boldsymbol{\tau}) = \boldsymbol{B}^{\dagger}$ to (26) does not depend on $\boldsymbol{\tau}$ since $\gamma_{2,k}$ and $\mathcal{C}_{\boldsymbol{B}}$ do not depend on $\boldsymbol{\tau}$. Therefore, the optimal transmit BF for problem (14) is obtained as $\boldsymbol{B}^o = \boldsymbol{B}^{\dagger}$.

Finally, the time allocation problem (21) is rewritten as

$$\max_{\boldsymbol{\tau}\in\mathcal{C}_{\boldsymbol{\tau}}} \min\{\tilde{\mathsf{R}}_1(\boldsymbol{\tau}), \tilde{\mathsf{R}}_2(\boldsymbol{\tau})\}, \quad (27)$$

where $\tilde{\mathsf{R}}_1(\boldsymbol{\tau}) = \mathsf{R}_1(\boldsymbol{w}^{\dagger}, \boldsymbol{\tau})$ and $\tilde{\mathsf{R}}_2(\boldsymbol{\tau}) = \mathsf{R}_2(\boldsymbol{B}^{\dagger}, \boldsymbol{\tau})$ denote the optimal values of (22) and (25), respectively.

In the following, we solve subproblems (24), (26), and (27) sequentially to obtain the optimal solution to problem (14).

A. ENERGY BF OPTIMIZATION

This subsection solves the energy BF optimization problem (24) by transforming it into

$$\max_{\boldsymbol{w}\in\mathcal{C}_{\boldsymbol{w}}, t\in\mathbb{R}_+} t \quad (28a)$$

$$\text{s.t. } \beta_k^2 |\boldsymbol{h}_k^T \boldsymbol{w}|^2 \ge t, \quad \forall k. \quad (28b)$$

It is well known that (28) has no closed-form solution [32] so that several algorithms finding an approximate solution have been developed; semi-definite relaxation (SDR) with randomization [32], [36], successive convex approximation (SCA) [33], and iterative algorithms [34], [35]. For the network with $M \ge 2K$, we propose to apply a linear combination of the orthogonal MF beams as

$$\boldsymbol{w} = \sum_{k=1}^{r(\boldsymbol{H})} q_k \boldsymbol{u}_k^* = \boldsymbol{U}^* \boldsymbol{q}, \quad (29)$$

where $\boldsymbol{q} = [q_1, q_2, \cdots, q_{r(\boldsymbol{H})}]^T \in \mathbb{C}^{r(\boldsymbol{H})}$ is a complex-valued weight vector and $\boldsymbol{U} = [\boldsymbol{u}_1, \boldsymbol{u}_2, \cdots, \boldsymbol{u}_{r(\boldsymbol{H})}]$ is an orthonormal basis of the column space of $\boldsymbol{H}$ satisfying $\boldsymbol{U}^H \boldsymbol{U} = \boldsymbol{I}_{r(\boldsymbol{H})}$. The optimization of $\boldsymbol{q}$ is equivalent to the optimization of $\boldsymbol{w}$ from Property 1.

Property 1: The solution to (28) lies in the column space of $\boldsymbol{H}^*$.

Proof: This result can be proved by contradiction. Assume that $\boldsymbol{w} = \boldsymbol{U}^* \boldsymbol{q} + \boldsymbol{e}$, where $\boldsymbol{e}$ is orthogonal to $\boldsymbol{U}^*$. The constraints in (28b) then become $\beta_k^2 |\boldsymbol{h}_k^T \boldsymbol{U}^* \boldsymbol{q}|^2 \ge t$, $\forall k$, and $\|\boldsymbol{q}\|^2 + \|\boldsymbol{e}\|^2 = 1$. Let $\boldsymbol{q}_{\varepsilon}$ be a vector satisfying $\|\boldsymbol{q}_{\varepsilon}\|^2 = 1 - \varepsilon$ for $\varepsilon = \|\boldsymbol{e}\|^2$ and $0 \le \varepsilon \le 1$. If we express $\boldsymbol{q}_{\varepsilon} = \sqrt{1-\varepsilon}\boldsymbol{q}_0$, we have $|\boldsymbol{h}_k^T \boldsymbol{U}^* \boldsymbol{q}_0|^2 \ge |\boldsymbol{h}_k^T \boldsymbol{U}^* \boldsymbol{q}_{\varepsilon}|^2$.

To make t as large as possible, we should have $\varepsilon = 0$, or equivalently $\boldsymbol{e} = \mathbf{0}_M$. □

From Property (1), problem (28) is now stated as

$$\max_{\boldsymbol{q}\in\mathcal{C}_{\boldsymbol{q}},t\in\mathbb{R}_+} \quad t, \tag{30a}$$

$$\text{s.t. } \beta_k^2|\boldsymbol{h}_k^T\boldsymbol{U}^*\boldsymbol{q}|^2 \geq t, \quad \forall k \tag{30b}$$

with $\mathcal{C}_{\boldsymbol{q}} = \{\boldsymbol{q}|\boldsymbol{q} \in \mathbb{C}^{r(\boldsymbol{H})}, \|\boldsymbol{q}\|^2 = 1\}$, of which the optimal solution $(\boldsymbol{q}^\dagger, t^\dagger)$ is obtained by applying one of the algorithms developed in [32]–[36] to lower the complexity of solving (28) with the generic BF vector $\boldsymbol{w} \in \mathbb{C}^M$; if the SDR with randomization [32] is applied to solve (28) and (30) for instance, the computational complexity is given by $O\left((2K+M^2)^{3.5}\right)$ to solve (28) and $O\left((2K+K^2)^{3.5}\right)$ to solve (30) with $r(\boldsymbol{H}) = 2K$.

When only a single device pair is served in the network, or equivalently when $K = 1$, we derive the closed-form solution $\boldsymbol{q}^\dagger$ to (30) in Appendix, which leads to

$$\boldsymbol{w}^\dagger = \begin{cases} e^{j\theta_1}\dfrac{\boldsymbol{h}_1^*}{\|\boldsymbol{h}_1\|}, & \text{if } \zeta_1 \leq 0, \\ e^{j\theta_1}\dfrac{\boldsymbol{h}_2^*}{\|\boldsymbol{h}_2\|}, & \text{if } \zeta_2 \leq 0, \\ e^{j\theta_1}\dfrac{\zeta_2\boldsymbol{h}_1^* + e^{j\angle\boldsymbol{h}_1^H\boldsymbol{h}_2}\zeta_1\boldsymbol{h}_2^*}{\sqrt{\det(\boldsymbol{H}^H\boldsymbol{H})(\beta_1\zeta_1+\beta_2\zeta_2)}}, & \text{if } \zeta_1,\zeta_2 > 0, \end{cases} \tag{31}$$

where θ_1 is an arbitrary phase, $\angle\cdot$ denotes the phase of a complex number,

$$\zeta_1 = \beta_1\|\boldsymbol{h}_1\|^2 - \beta_2|\boldsymbol{h}_1^H\boldsymbol{h}_2|, \tag{32}$$

and

$$\zeta_2 = \beta_2\|\boldsymbol{h}_2\|^2 - \beta_1|\boldsymbol{h}_1^H\boldsymbol{h}_2|. \tag{33}$$

The solution (31) leads to the optimal value $t^\dagger$ of (30) when $K = 1$ as

$$t^\dagger = \begin{cases} \beta_1^2\|\boldsymbol{h}_1\|^2, & \text{if } \zeta_1 \leq 0, \\ \beta_2^2\|\boldsymbol{h}_2\|^2, & \text{if } \zeta_2 \leq 0, \\ \dfrac{\beta_1^2\beta_2^2\det(\boldsymbol{H}^H\boldsymbol{H})}{\beta_1^2\|\boldsymbol{h}_1\|^2 - 2\beta_1\beta_2|\boldsymbol{h}_1^H\boldsymbol{h}_2| + \beta_2^2\|\boldsymbol{h}_2\|^2} & \text{if } \zeta_1,\zeta_2 > 0. \end{cases} \tag{34}$$

The optimal value $\gamma_1^\dagger$ of the MAC SNR (23) is then expressed as

$$\gamma_1^\dagger = \eta\frac{\tau_0}{\tau_1}\frac{\mathsf{P}_\mathrm{H}}{\sigma_1^2}t^\dagger = \frac{\tau_0}{\tau_1}\tilde{\gamma}_1^\dagger, \tag{35}$$

where $\tilde{\gamma}_1^\dagger = \eta\frac{\mathsf{P}_\mathrm{H}}{\sigma_1^2}t^\dagger$ is the time-independent factor of the optimal MAC SNR; for $K = 1$, the optimal value $t^\dagger$ of (30) is obtained with (34); for $K > 1$, it is obtained by applying one of the algorithms described after (30). Finally, the optimal value of (22) is expressed as

$$\tilde{\mathsf{R}}_1(\boldsymbol{\tau}) = \tau_1\log_2\left(1+\frac{\tau_0}{\tau_1}\tilde{\gamma}_1^\dagger\right). \tag{36}$$

B. TRANSMIT BF OPTIMIZATION

This subsection solves the transmit BF optimization problem (26) by decomposing it into pairwise BF and inter-pair power allocation problems from an observation that the SNRs $\gamma_{2,2p-1}$ and $\gamma_{2,2p}$ of the pth pair depend only on $\boldsymbol{b}_p$. For this purpose, we express the pairwise BF vector as $\boldsymbol{b}_p = \lambda_p\tilde{\boldsymbol{b}}_p$ subject to $\|\tilde{\boldsymbol{b}}_p\|^2 = 1$ and $\lambda_p \geq 0$ and construct the power allocation vector $\boldsymbol{\lambda} = [\lambda_1, \lambda_2, \cdots, \lambda_K]^T$ subject to $\sum_{p=1}^K \lambda_p = 1$. After removing the irrelevant factors in the SNR (13), we can then rewrite (26) as

$$\max_{\boldsymbol{\lambda}} \min_{1\leq p\leq K} \lambda_p \left\{ \max_{\tilde{\boldsymbol{b}}_p} \min\left(|\boldsymbol{g}_{2p-1}^T\tilde{\boldsymbol{b}}_p|^2, |\boldsymbol{g}_{2p}^T\tilde{\boldsymbol{b}}_p|^2\right)\right\} \tag{37a}$$

$$\text{s.t. } \tilde{\boldsymbol{b}}_p \in \mathcal{C}_{\tilde{\boldsymbol{b}}_p}, \quad p = 1, 2, \cdots, K, \ \boldsymbol{\lambda} \in \mathcal{C}_{\boldsymbol{\lambda}}, \tag{37b}$$

where $\mathcal{C}_{\tilde{\boldsymbol{b}}_p} = \{\tilde{\boldsymbol{b}}_p|\tilde{\boldsymbol{b}}_p \in \mathbb{C}^L, \|\tilde{\boldsymbol{b}}_p\|^2 = 1\}$ and $\mathcal{C}_{\boldsymbol{\lambda}} = \{\boldsymbol{\lambda}|\boldsymbol{\lambda} \in \mathbb{R}_+^K, \sum_{p=1}^K \lambda_p = 1\}$.

We now solve problem (37) by optimizing the normalized pairwise BF as

$$\max_{\tilde{\boldsymbol{b}}_p\in\mathcal{C}_{\tilde{\boldsymbol{b}}_p}} \min\left(|\boldsymbol{g}_{2p-1}^T\tilde{\boldsymbol{b}}_p|^2, |\boldsymbol{g}_{2p}^T\tilde{\boldsymbol{b}}_p|^2\right) \tag{38}$$

and then optimizing the inter-pair power allocation $\boldsymbol{\lambda}$ with the optimal value $s_p^\dagger$ of (38) as

$$\max_{\boldsymbol{\lambda}\in\mathcal{C}_{\boldsymbol{\lambda}}} \left\{ \min_{1\leq p\leq K} \lambda_p s_p^\dagger\frac{\mathsf{P}_\mathrm{H}}{\sigma^2}\right\}. \tag{39}$$

Problem (38) can now be transformed into

$$\max_{\tilde{\boldsymbol{b}}_p\in\mathcal{C}_{\tilde{\boldsymbol{b}}_p}, s_p\in\mathbb{R}_+} \quad s_p \tag{40a}$$

$$\text{s.t. } |\boldsymbol{g}_k^T\tilde{\boldsymbol{b}}_p|^2 \geq s_p, \quad k = 2p-1, 2p, \tag{40b}$$

which is a special case of (28) when $K = 1$ and $\beta_k = 1$. Therefore, the closed-form solution to (40) is obtained as

$$\tilde{\boldsymbol{b}}_p^\dagger = \begin{cases} e^{j\theta_p}\dfrac{\boldsymbol{g}_{2p-1}^*}{\|\boldsymbol{g}_{2p-1}\|}, & \text{if } \tilde{\zeta}_{2p-1} \leq 0, \\ e^{j\theta_p}\dfrac{\boldsymbol{g}_{2p}^*}{\|\boldsymbol{g}_{2p}\|}, & \text{if } \tilde{\zeta}_{2p} \leq 0, \\ e^{j\theta_p}\dfrac{\tilde{\zeta}_{2p}\boldsymbol{g}_{2p-1}^* + e^{j\angle\boldsymbol{g}_{2p-1}^H\boldsymbol{g}_{2p}}\tilde{\zeta}_{2p-1}\boldsymbol{g}_{2p}^*}{\sqrt{\det(\boldsymbol{G}_p^H\boldsymbol{G}_p)(\tilde{\zeta}_{2p-1}+\tilde{\zeta}_{2p})}}, \\ \qquad\qquad \text{if } \tilde{\zeta}_{2p-1}, \tilde{\zeta}_{2p} > 0 \end{cases} \tag{41}$$

where θ_p is an arbitrary phase, $\boldsymbol{G}_p = [\boldsymbol{g}_{2p-1}, \boldsymbol{g}_{2p}]$,

$$\tilde{\zeta}_{2p-1} = \|\boldsymbol{g}_{2p-1}\|^2 - |\boldsymbol{g}_{2p-1}^H\boldsymbol{g}_{2p}|, \tag{42}$$

and

$$\tilde{\zeta}_{2p} = \|\boldsymbol{g}_{2p}\|^2 - |\boldsymbol{g}_{2p-1}^H\boldsymbol{g}_{2p}|. \tag{43}$$

The optimal value of (40) is also expressed as

$$s_p^\dagger = \begin{cases} \|\boldsymbol{g}_{2p-1}\|^2, & \text{if } \tilde{\zeta}_{2p-1} \leq 0, \\ \|\boldsymbol{g}_{2p}\|^2, & \text{if } \tilde{\zeta}_{2p} \leq 0, \\ \dfrac{\det(\boldsymbol{G}_p^H\boldsymbol{G}_p)}{\mathrm{tr}(\boldsymbol{G}_p^H\boldsymbol{G}_p) - 2|\boldsymbol{g}_{2p-1}^H\boldsymbol{g}_{2p}|}, & \text{if } \tilde{\zeta}_{2p-1}, \tilde{\zeta}_{2p} > 0. \end{cases} \tag{44}$$

In the meantime, the solution $\boldsymbol{\lambda}^\dagger$ to (39) is given by

$$\lambda_p^\dagger = \frac{1}{s_p^\dagger}\left(\sum_{l=1}^{K}\frac{1}{s_l^\dagger}\right)^{-1} \tag{45}$$

since (39) is maximized when $\lambda_1 s_1^\dagger = \lambda_2 s_2^\dagger = \cdots = \lambda_K s_K^\dagger$. From the results (39) and (45), the optimal value of (26) is expressed as

$$\gamma_2^\dagger = \frac{\mathsf{P}_\mathrm{H}}{\sigma^2}\left(\sum_{l=1}^{K}\frac{1}{s_l^\dagger}\right)^{-1} \tag{46}$$

with which the optimal value of (25) is given by

$$\tilde{\mathsf{R}}_2(\boldsymbol{\tau}) = \tau_2 \log_2(1+\gamma_2^\dagger). \tag{47}$$

C. TIME ALLOCATION OPTIMIZATION

We finally solve the time allocation problem (27) which is expressed more explicitly with (36) and (47) as

$$\max_{\boldsymbol{\tau}\in\mathcal{C}_{\boldsymbol{\tau}}} \ \min\left\{\tau_1 \log_2\left(1+\frac{\tau_0}{\tau_1}\tilde{\gamma}_1^\dagger\right), \tau_2\log_2(1+\gamma_2^\dagger)\right\}. \tag{48}$$

By introducing a new variable ς, (48) is now transformed into

$$\max_{\boldsymbol{\tau}\in\mathcal{C}_{\boldsymbol{\tau}},\varsigma\in\mathbb{R}_+} \ \varsigma \tag{49a}$$

$$\text{s.t. } \varsigma - \tau_1\log_2\left(1+\frac{\tau_0}{\tau_1}\tilde{\gamma}_1^\dagger\right) \le 0, \tag{49b}$$

$$\varsigma - \tau_2\log_2(1+\gamma_2^\dagger) \le 0. \tag{49c}$$

This problem is shown to be convex with the linear objective function (49a), linear constraints $\mathcal{C}_{\boldsymbol{\tau}}$ and (49c), and convex constraint (49b). The convexity of (49b) is confirmed by investigating the Hessian

$$\nabla^2\tilde{\mathsf{R}}_1(\tau_0,\tau_1) = \frac{(\tilde{\gamma}_1^\dagger)^2}{(\tau_1+\tau_0\tilde{\gamma}_1^\dagger)^2\ln 2}\begin{bmatrix}-\tau_1 & \tau_0\\ \tau_0 & -\dfrac{\tau_0^2}{\tau_1}\end{bmatrix} \tag{50}$$

of $\tilde{\mathsf{R}}_1(\tau_0,\tau_1) = \tau_1\log_2\left(1+\frac{\tau_0}{\tau_1}\tilde{\gamma}_1^\dagger\right)$. Clearly, $\tilde{\mathsf{R}}_1(\tau_0,\tau_1)$ is concave with the negative semi-definite Hessian so that the left-hand side of (49b) is convex. Therefore, we can solve problem (49) with existing convex optimization solvers [39].

IV. NUMERICAL RESULTS

We evaluate the performance of the network by assuming $\mathsf{P}_\mathrm{H} = 1$ W and $\sigma_1^2 = -110$ dBm for the transmit power and noise power of a high-cost HAP, respectively and $\sigma_2^2 = -90$ dBm and $\eta = 0.5$ for the noise power and energy harvesting efficiency of low-cost devices, respectively. In this evaluation, the path loss of the Rayleigh fading channels is set to $\omega_k = 0.001\, d_k^{-2.5}$, where d_k is the distance between the HAP and D_k for $k = 1, 2, \cdots, 2K$.

Before evaluating the overall max-min rate performance, we compare the performance of the BF methods in Figs. 2-4 by evaluating the minimum SNR, $\gamma_1 = \min_{1\le k\le 2K}\gamma_{1,k}$ with $\tau_0/\tau_1 = 1$ for the MAC phase and $\gamma_2 = \min_{1\le k\le 2K}\gamma_{2,k}$ for the BC phase. In the figures, the devices are located at $d_{2p-1} = 15$ m and $d_{2p} = 25$ m for $p = 1, 2, \cdots, K$.

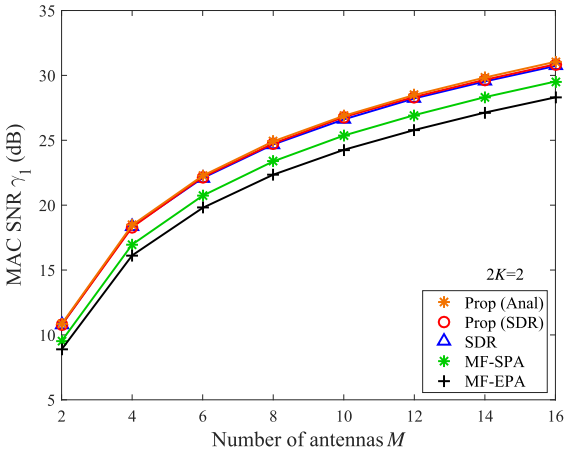

FIGURE 2. Minimum SNR γ_1 in the MAC phase with $2K = 2$ as the number of antennas M varies.

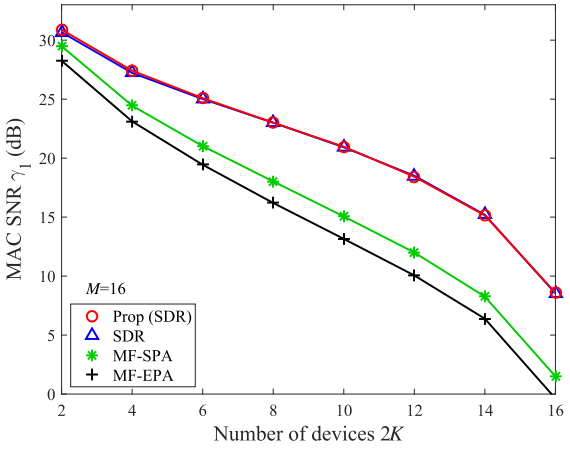

FIGURE 3. Minimum SNR γ_1 in the MAC phase with $M = 16$ as the number of devices $2K$ varies.

Fig. 2 compares the energy BF methods for two devices $2K = 2$ versus the number of antennas M. In the figure, 'Prop (Anal)' denotes the analytically derived optimal energy BF (31) whilst 'Prop (SDR)' and 'SDR' denote the energy BF obtained by solving (30) and (28), respectively, through the SDR with randomization [32], [36] generating 3000 candidates for the randomization method randC in [32]. For the benchmark, we also compare the performance of the conventional MF-based energy BF, formed by a linear combination of the MF beams with real-valued weights [10], [22]; 'MF-SPA' denotes the MF-based energy BF with asymptotically optimal weights obtained by assuming a large number of antennas [10] and 'MF-EPA' denotes the MF-based energy BF with equal-valued weights [22]. Apparently, the minimum SNR in the MAC increases with the number of antennas when the number of devices is fixed. In the figure, 'Prop (Anal)' with the exact closed-form solution slightly outperforms 'Prop (SDR)' and 'SDR', which correspond to approximate

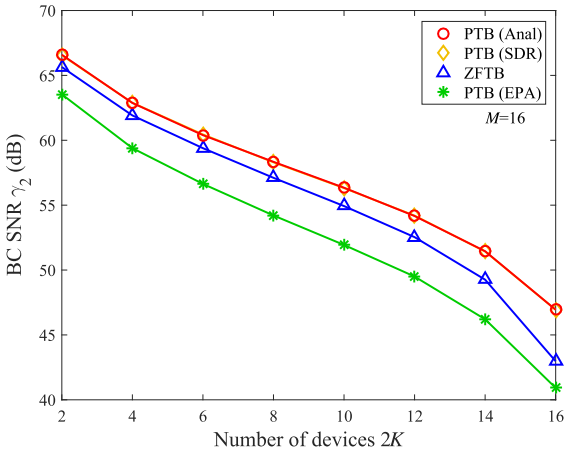

FIGURE 4. Minimum SNR γ_2 in the BC phase with $M = 16$ as the number of devices $2K$ varies.

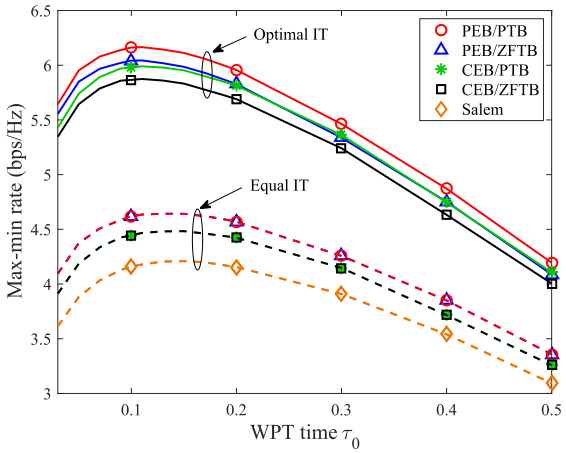

FIGURE 5. Max-min rate as a function of τ_0 when $M = 2K = 2$ and $d_k = 5$ m.

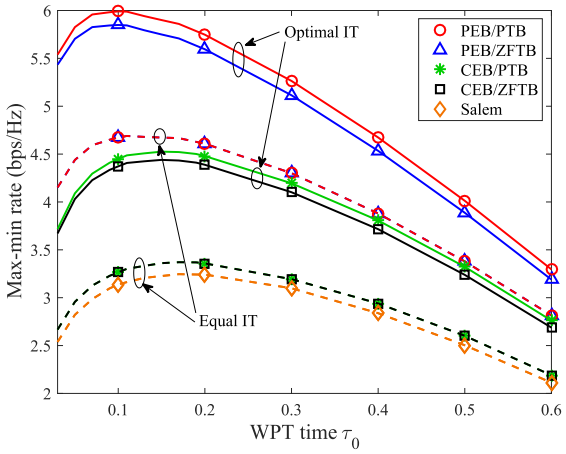

FIGURE 6. Max-min rate as a function of τ_0 when $M = 2K = 16$ and $d_k = 5$ m.

solutions obtained at a higher complexity. Meanwhile, 'Prop (Anal)' evidently outperforms the conventional 'MF-SPA' and 'MF-EPA' methods which are computed at a comparable complexity.

The energy BF methods are also compared in Fig. 3 as the number of devices $2K$ increases while fixing the number of antennas as $M = 16$. In the figure, the results of 'Prop (Anal)' are not shown since they are not available for $2K > 2$. Again, the performances of 'Prop (SDR)' and 'SDR' are almost indistinguishable, which implies 'Prop (SDR)' could replace 'SDR' without performance loss to lower the computational complexity, as delineated in Subsection III-A. It is obvious that, for a fixed number of antennas, the minimum SNR in the MAC decreases as the number of devices increases. It is also observed that the proposed energy BF outperforms the conventional 'MF-SPA' and 'MF-EPA' methods significantly, where the gain becomes larger as the number of devices increases.

Under the same conditions as in Fig. 3, the minimum SNR γ_2 in the BC phase is also shown in Fig. 4 as the number of devices varies. In the figure, 'PTB (Anal)' and 'PTB (SDR)' indicate the proposed two-step transmit BF of which the second-step pairwise BF is obtained from the analysis and the SDR algorithm, respectively. Meanwhile, 'ZFTB' denotes the conventional ZF for the transmission of $2K$ decoded symbols without network coding. The figure confirms the validity of 'PTB (Anal)' which provides an indistinguishable performance from 'PTB (SDR)' without resorting to an optimization algorithm. The gain of 'PTB' over 'ZFTB' becomes larger as $2K$ increases since 'PTB' and 'ZFTB' exploit the diversity gains of $M - 2K + 2$ and $M - 2K + 1$, respectively, by nulling the interferences from $2K - 2$ and $2K - 1$ devices, respectively, using M antennas. It should be noted that the BC performance in Fig. 4 is much better than the MAC performance in Fig. 3 since the former suffers from a single path loss for the donwlink BC while the latter suffers from a double path loss for the uplink MAC combined with the downlink WPT. Therefore, appropriate time allocation into the MAC and BC phases would help WP-TWR to improve the rate performance determined by the minimum rate of the MAC and BC phases.

The max-min rate of the multi-pair WP-TWR protocol is shown as a function of the WPT time τ_0 in Figs. 5 and 6 when the devices are equidistant at $d_k = 5$ m. We set $M = 2K = 2$ in Fig. 5 and $M = 2K = 16$ in Fig. 6, where 'PEB/PTB', 'PEB/ZFTB', 'CEB/PTB', and 'CEB/ZFTB' denote different energy and transmit BF methods of DF-based WP-TWR; 'PEB' and 'CEB' denote the energy BF with 'Prop (SDR)' ('Prop (Anal)' for $2K = 2$) and with the conventional 'MF-SPA', respectively, and 'PTB' and 'ZFTB' denote the proposed two-step TB in closed-form and the conventional ZF transmitting $2K$ symbols without network coding, respectively. In the figure, we consider the performance of two time allocation methods: 'Optimal IT' optimizes the time allocation (τ_1, τ_2) for a given τ_0 and 'Equal IT' sets $\tau_1 = \tau_2 = \frac{1-\tau_0}{2}$ for a given τ_0. In addition, 'Salem' denotes the AF-based WP-TWR with ZF BF proposed in [22], for which only 'Equal IT' is possible.

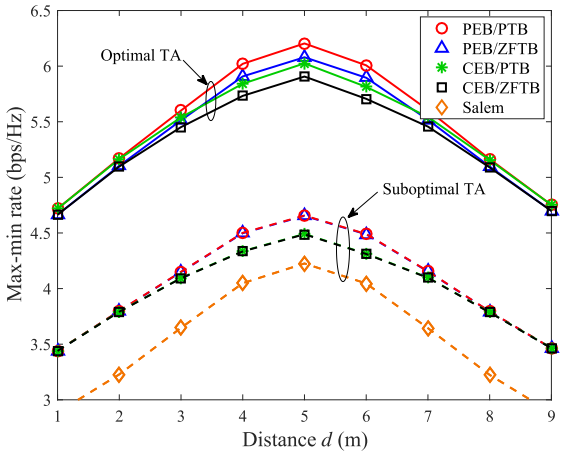

FIGURE 7. Max-min rate as a function of distance d when $M = 2K = 2$.

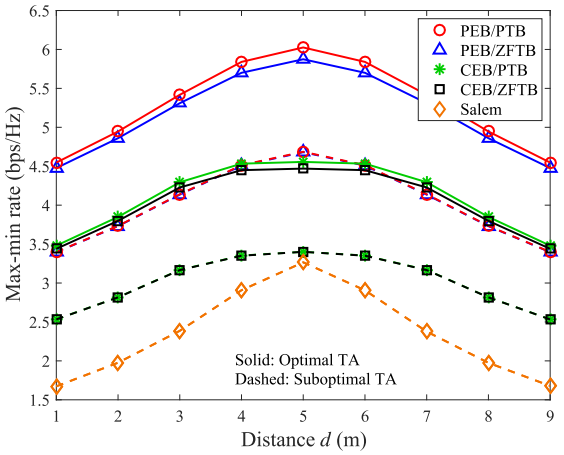

FIGURE 8. Max-min rate as a function of distance d when $M = 2K = 16$.

Clearly, the DF-based WP-TWR protocols outperform the AF-based one ('Salem') significantly in Figs. 5-6 by allowing flexible time allocation to the MAC and BC phases exhibiting imbalanced performance. Even with 'Equal IT', the DF-based methods exhibit performance gains over the AF-based method by employing a better energy BF method and avoiding the noise amplification incurred by the AF. This noise amplification is larger in the WP-TWR than in the traditional TWR since the MAC SNR of the WP-TWR experiences double path loss in the course of energy harvesting and information transfer. Among the DF-based methods, 'PEB/PTB' with 'Optimal IT' provides the best performance for all τ_o by improving the MAC and BC performances with the proposed BF methods and balancing the performance of the MAC and BC phases adequately with the time allocation. With 'Equal IT', the performance of 'PTB' and 'ZFTB' for the given energy BF becomes indistinguishable since the MAC phase dominates the performance with equal time allocation for the MAC and BC phases. It is also observed in Figs. 5-6 that optimal time allocation is more beneficial to the performance than the proposed BF for $K = 1$ while the proposed BF is more beneficial for $2K = 16$. This observation arises from the fact that the energy BF adapts $2K$ complex-valued weights to attain max-min fairness among the $2K$ devices while the time allocation adapts only three time variables, irrespective of the number of devices.

The max-min rate is now shown as a function of distance d (m) in Figs. 7 and 8 when $d_{2p-1} = d$ and $d_{2p} = 10 - d$ for $p = 1, 2, \cdots, K$. We set $M = 2K = 2$ in Fig. 7 and $M = 2K = 16$ in Fig. 8, where 'Optimal TA' denotes the performance after optimizing $\boldsymbol{\tau} = [\tau_0, \tau_1, \tau_2]$ in (49) and 'Suboptimal TA' denotes the performance after optimizing the WPT time τ_0 for $\tau_1 = \tau_2$ ('Equal IT'). The best performance is achieved at the center location of the HAP providing the balanced performance of the bidirectional data flows. The performance gaps among the schemes in Figs. 7 and 8 are similar to those in Figs. 5 and 6, respectively, except that the gaps vary with location.

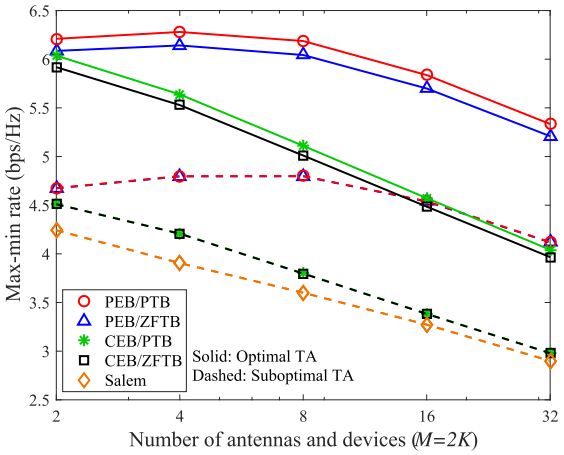

FIGURE 9. Max-min rate as a function of the number of antennas and devices ($M = 2K$) when $d_k = 5$ m.

Fig. 9 provides the max-min rate as a function of the number of antennas M when $M = 2K$, i.e., the number of antennas is equal to the number of devices, and the devices are equidistant as $d_k = 5$ m. The max-min rate $\mathsf{R}_{\min}$ of each device tends to decrease in general as the number of antennas increases, although the total rate $2K\mathsf{R}_{\min}$ supported by the network increases. The gain of the proposed 'PEB' over 'CEB' for the energy BF gets larger as both the number of antennas and the number of devices increase since 'PEB' adapts to the multi-user channels better than 'CEB'. The optimal time allocation also provides a significant gain, which tends to be larger with a smaller number of devices, where the BF gain is rather smaller. It is clear that the proposed 'PEB/PTB' provides the best performance among the schemes considered. Notably, various combinations of the energy BF, transmit BF, and time allocation methods for the proposed DF-based WP-TWR network outperform the conventional AF-based WP-TWR network, which provides more flexibility in the network design by trading off the computation complexity and the performance.

V. CONCLUSION

We have considered a multi-pair WP-TWR network in which a multi-antenna HAP transfers the power to the devices and assists the data exchange in three phases. For the efficient multi-pair TWR, we have applied the DF with network coding with flexible time allocation and the two-step transmit BF that steers the beams toward the network coding device pairs while avoiding the inter-pair interference. We have formulated the problem as maximizing the rate fairness among the devices by optimizing energy BF and transmit BF while considering three-phase time allocation. This problem was solved by formulating an equivalent problem consisting of three subproblems: independent optimization of the energy and transmit BFs for a given time allocation, and optimization of the time allocation with the optimized BFs. The energy BF was derived in closed-form for the case of two devices, and was searched for in the span of the channel matched filters at a lower complexity by adopting the existing algorithms for the other cases. The transmit BF was derived in closed-form with the readily available pairwise BF and inter-pair power allocation, and the time allocation problem was solved via an existing convex optimization solver after demonstrating the convexity of the problem. The results showed that the proposed WP-TWR network outperforms the conventional AF-based one by employing the enhanced BF and flexible time allocation methods.

The proposed WP-TWR network supporting two devices is implementable at rather low complexity. If more than two devices are supported, optimization of the energy BF required for the proposed network can be handled by the HAP at a complexity comparable to that of the APs since recent APs are being developed to possess various levels of computing power for fog and edge computing. In addition, the proposed network enables various combinations of the optimal and suboptimal methods in energy BF and time allocation according the complexity and performance requirements under the designer's discretion. Furthermore, the proposed independently designed BF methods are applicable to other protocols, such as the proposed energy BF to wireless powered uplink and one-way relay, and the proposed transmit BF to multi-way relay with network coding. In this context, the HAP of the proposed WP-TWR network can be extended to a universal power-supply and radio-access platform that supports all the aforementioned protocols to facilitate various IoT communications.

APPENDIX

To solve problem (30) for $K = 1$, we first express the channel vectors using an orthonormal basis $\{\boldsymbol{u}_i\}$ as $\boldsymbol{h}_i = a_{i1}\boldsymbol{u}_1 + a_{i2}\boldsymbol{u}_2$, where $a_{ij} = \boldsymbol{u}_j^H \boldsymbol{h}_i$. An orthonormal basis can be obtained via the Gram-Schmidt orthogonalization process as

$$\boldsymbol{u}_1 = \frac{\boldsymbol{h}_1}{\|\boldsymbol{h}_1\|}, \quad \boldsymbol{u}_2 = \frac{\boldsymbol{h}_2 - \boldsymbol{u}_1^H \boldsymbol{h}_2 \boldsymbol{u}_1}{\|\boldsymbol{h}_2 - \boldsymbol{u}_1^H \boldsymbol{h}_2 \boldsymbol{u}_1\|}, \tag{51}$$

which leads to the coefficients

$$a_{11} = \|\boldsymbol{h}_1\|, \ a_{12} = 0, \tag{52}$$

$$a_{21} = \frac{\boldsymbol{h}_1^H \boldsymbol{h}_2}{\|\boldsymbol{h}_1\|}, \quad a_{22} = \frac{\sqrt{\det(\boldsymbol{H}^H \boldsymbol{H})}}{\|\boldsymbol{h}_1\|}. \tag{53}$$

We now rewrite problem (30) as

$$\max_{\boldsymbol{q}\in\mathbb{C}^2, t\in\mathbb{R}_+} \quad t \tag{54a}$$

$$\text{s.t.} \ \ \beta_1^2 |a_{11}|^2 |q_1|^2 \geq t, \tag{54b}$$

$$\beta_2^2 \left(\sum_{i=1}^{2} |a_{2i}|^2 |q_i|^2 + 2\Re\{a_{21} a_{22}^* q_1 q_2^*\} \right) \geq t, \tag{54c}$$

$$|q_1|^2 + |q_2|^2 = 1, \tag{54d}$$

where $\Re\{\cdot\}$ denotes the real part of a complex value. By expressing $\boldsymbol{q} = (r_1 e^{j\theta_1}, r_2 e^{j\theta_2})$ in polar coordinate, we now optimize problem (54) with amplitude $\boldsymbol{r} = (r_1, r_2)$ and phase $\boldsymbol{\theta} = (\theta_1, \theta_2)$ as

$$\max_{\boldsymbol{r}\in\mathbb{R}_+^2, \boldsymbol{\theta}\in[0,2\pi)^2, t\in\mathbb{R}_+} \quad t \tag{55a}$$

$$\text{s.t.} \ \ \beta_1^2 |a_{11}|^2 r_1^2 \geq t, \tag{55b}$$

$$\beta_2^2 \left(\sum_{i=1}^{2} |a_{2i}|^2 r_i^2 + 2\Re\{a_{21} a_{22}^* e^{j(\theta_1 - \theta_2)}\} r_1 r_2 \right) \geq t, \tag{55c}$$

$$r_1^2 + r_2^2 = 1. \tag{55d}$$

The optimal phases are found easily since only constraint (55c) depends on $\boldsymbol{\theta}$. To maximize t, we should maximize the left hand side of (55c), and the maximum is obtained when the phase difference $\theta_{21} = \theta_2 - \theta_1$ satisfies

$$\theta_{21}^{\dagger} = \angle(a_{21} a_{22}^*) = \angle(\boldsymbol{h}_1^H \boldsymbol{h}_2) \tag{56}$$

for a given $\boldsymbol{r}$. With the optimum phases, constraint (55c) becomes an indefinite quadratic form as

$$\beta_2^2 \left(|a_{21}| r_1 + |a_{22}| r_2 \right)^2 \geq t. \tag{57}$$

By defining $\tilde{t} = \sqrt{t}$, we transform the problem (55) into

$$\max_{\boldsymbol{r}\in\mathbb{R}_+^2, \tilde{t}\in\mathbb{R}_+} \quad \tilde{t} \tag{58a}$$

$$\text{s.t.} \ \ \beta_1 |a_{11}| r_1 \geq \tilde{t}, \tag{58b}$$

$$\beta_2 \left(|a_{21}| r_1 + |a_{22}| r_2 \right) \geq \tilde{t}, \tag{58c}$$

$$r_1^2 + r_2^2 = 1. \tag{58d}$$

By removing the equality constraint (58d), we have

$$\max_{0\leq r_1 \leq 1, \tilde{t}\in\mathbb{R}_+} \quad \tilde{t} \tag{59a}$$

$$\text{s.t.} \ \ f_1(r_1) \geq \tilde{t}, \quad f_2(r_1) \geq \tilde{t}, \tag{59b}$$

where

$$f_1(r_1) = \beta_1 |a_{11}| r_1 \tag{60}$$

and

$$f_2(r_1) = \beta_2 \left(|a_{21}| r_1 + |a_{22}| \sqrt{1 - r_1^2} \right). \tag{61}$$

Clearly, problem (59) is a convex optimization problem having a unique optimum solution since the objective function is linear and the constraints are convex with the linear function $f_1(r_1)$ and concave function $f_2(r_1)$ satisfying $f_2''(r_1) > 0$. Here, $f_1(r_1)$ is linearly increasing in $r_1 \in [0, 1]$ with the maximum at $r_1 = 1$ while $f_2(r_1)$ is concave with the unique maximum at $r_1 = r_1^{c2}$, where

$$r_1^{c2} = \frac{|a_{21}|}{\sqrt{|a_{21}|^2 + |a_{22}|^2}} = \frac{|\boldsymbol{h}_1^H \boldsymbol{h}_2|}{\|\boldsymbol{h}_1\| \|\boldsymbol{h}_2\|}. \tag{62}$$

Noting that $f_1(r_1)$ and $f_2(r_1)$ have no intersections or a unique intersection according to the channel realizations, we derive the optimal solution to (59) as follows:

Case 1) If $f_1(1) \leq f_2(1)$, or equivalently

$$\zeta_1 = \beta_1 \|\boldsymbol{h}_1\|^2 - \beta_2 |\boldsymbol{h}_1^H \boldsymbol{h}_2| \leq 0, \tag{63}$$

$f_1(r_1)$ and $f_2(r_1)$ have no intersections in $r_1 \in [0, 1]$. In this case, the maximum $\tilde{t}^\dagger$ of $\tilde{t}$ occurs at $r_1^\dagger = 1$ as $\tilde{t}^\dagger = f_1(1)$.

Case 2) If $f_1(1) > f_2(1)$ (that is, $\zeta_1 > 0$) and $f_1(r_1^{c2}) \geq f_2(r_1^{c2})$, or equivalently

$$\zeta_2 = \beta_2 \|\boldsymbol{h}_2\|^2 - \beta_1 |\boldsymbol{h}_1^H \boldsymbol{h}_2| \leq 0, \tag{64}$$

the maximum $\tilde{t}^\dagger$ occurs at $r_1^\dagger = r_1^{c2}$ as $\tilde{t}^\dagger = f_2(r_1^{c2})$.

Case 3) If $f_1(1) > f_2(1)$, or equivalently $\zeta_1 > 0$, and $f_1(r_1^{c2}) < f_2(r_1^{c2})$, or equivalently $\zeta_2 > 0$, the maximum $\tilde{t}^\dagger$ occurs at the unique intersection of $f_1(r_1)$ and $f_2(r_1)$ in $r_1 \in [0, 1]$, which is given by

$$\begin{aligned} r_1^{c3} &= \frac{\beta_2 |a_{22}|}{\sqrt{\beta_2^2 |a_{22}|^2 + (\beta_1 |a_{11}| - \beta_2 |a_{21}|)^2}} \\ &= \frac{\beta_2 \sqrt{\det(\boldsymbol{H}^H \boldsymbol{H})}}{\|\boldsymbol{h}_1\| \sqrt{\beta_1 \zeta_1 + \beta_2 \zeta_2}}. \end{aligned} \tag{65}$$

Therefore, $\tilde{t}^\dagger = f_1(r_1^{c3}) = f_2(r_1^{c3})$.

Remark: The conditions for Case 2, $\zeta_1 > 0$ and $\zeta_2 \leq 0$, are simplified as $\zeta_2 \leq 0$ since the condition $\zeta_2 \leq 0$ is equivalent to the condition $\zeta_1 \geq 0$; From $\zeta_2 \leq 0$ ($\beta_2 \|\boldsymbol{h}_2\|^2 \leq \beta_1 |\boldsymbol{h}_1^H \boldsymbol{h}_2|$) and the Cauchy-Schwarz inequality

$$\beta_1 |\boldsymbol{h}_1^H \boldsymbol{h}_2| \leq \beta_1 \|\boldsymbol{h}_1\| \|\boldsymbol{h}_2\|, \tag{66}$$

we have $\beta_2 \|\boldsymbol{h}_2\|^2 \leq \beta_1 \|\boldsymbol{h}_1\| \|\boldsymbol{h}_2\|$, or equivalently $\beta_2 \|\boldsymbol{h}_2\| \|\boldsymbol{h}_1\| \leq \beta_1 \|\boldsymbol{h}_1\|^2$ after multiplying $\|\boldsymbol{h}_1\| / \|\boldsymbol{h}_2\|$ to both sides. If we apply the Cauchy-Schwarz inequality again, we have

$$\beta_2 |\boldsymbol{h}_1^H \boldsymbol{h}_2| \leq \beta_2 \|\boldsymbol{h}_2\| \|\boldsymbol{h}_1\| \leq \beta_1 \|\boldsymbol{h}_1\|^2, \tag{67}$$

which is equivalent to $\zeta_1 \geq 0$. Therefore, the condition $\zeta_1 > 0$ is not required for Case 2. Using the same reasoning, the condition $\zeta_1 \leq 0$ implies that $\zeta_2 \geq 0$. Finally, the condition $\{\zeta_1 \leq 0, \zeta_2 \leq 0\}$ is not feasible.

Therefore, we can summarize as follows:

$$\boldsymbol{r}^\dagger = \begin{cases} [1, 0]^T, & \text{if } \zeta_1 \leq 0, \\ \left[\dfrac{|\boldsymbol{h}_1^H \boldsymbol{h}_2|}{\|\boldsymbol{h}_1\| \|\boldsymbol{h}_2\|}, \dfrac{\sqrt{\det(\boldsymbol{H}^H \boldsymbol{H})}}{\|\boldsymbol{h}_1\| \|\boldsymbol{h}_2\|} \right]^T, & \text{if } \zeta_2 \leq 0, \\ \dfrac{1}{\|\boldsymbol{h}_1\|} \left[\dfrac{\beta_2 \sqrt{\det(\boldsymbol{H}^H \boldsymbol{H})}}{\sqrt{\beta_1 \zeta_1 + \beta_2 \zeta_2}}, \dfrac{\zeta_1}{\sqrt{\beta_1 \zeta_1 + \beta_2 \zeta_2}} \right]^T, & \text{if } \zeta_1, \zeta_2 > 0. \end{cases} \tag{68}$$

With the optimal $\boldsymbol{r}^\dagger$ and $\theta_{21}^\dagger$, we have $\boldsymbol{q}^\dagger = [r_1^\dagger e^{j\theta_1}, r_2^\dagger e^{j(\theta_1 + \theta_{21}^\dagger)}]$ for an arbitrary phase θ_1, which leads to the optimal value $t^\dagger = (\tilde{t}^\dagger)^2$ provided in (34). The explicit expression for the optimal energy BF $\boldsymbol{w}^\dagger$ is also given in (31) from $\boldsymbol{w}^\dagger = e^{j\theta_1}(r_1^\dagger \boldsymbol{u}_1^* + r_2^\dagger e^{j\theta_{21}^\dagger} \boldsymbol{u}_1^*)$.

REFERENCES

[1] R. Zhang and C. K. Ho, "MIMO broadcasting for simultaneous wireless information and power transfer," *IEEE Trans. Wireless Commun.*, vol. 12, no. 5, pp. 1989–2001, May 2013.

[2] X. Zhou, R. Zhang, and C. K. Ho, "Wireless information and power transfer: Architecture design and rate-energy tradeoff," *IEEE Trans. Commun.*, vol. 61, no. 11, pp. 4754–4767, Nov. 2013.

[3] H. Ju and R. Zhang, "Throughput maximization in wireless powered communication networks," *IEEE Trans. Wireless Commun.*, vol. 13, no. 1, pp. 418–428, Jan. 2014.

[4] S. Bi, C. K. Ho, and R. Zhang, "Wireless powered communication: Opportunities and challenges," *IEEE Commun. Mag.*, vol. 53, no. 4, pp. 117–125, Apr. 2015.

[5] X. Lu, P. Wang, D. Niyato, D. I. Kim, and Z. Han, "Wireless networks with RF energy harvesting: A contemporary survey," *IEEE Commun. Surveys Tuts.*, vol. 17, no. 2, pp. 757–789, 2nd Quart., 2015.

[6] S. Bi, Y. Zeng, and R. Zhang, "Wireless powered communication networks: An overview," *IEEE Wireless Commun.*, vol. 23, no. 2, pp. 10–18, Apr. 2016.

[7] D. Niyato, D. I. Kim, M. Maso, and Z. Han, "Wireless powered communication networks: Research directions and technological approaches," *IEEE Wireless Commun.*, vol. 24, no. 6, pp. 88–97, Dec. 2017.

[8] T. D. P. Perera, D. N. K. Jayakody, S. K. Sharma, S. Chatzinotas, and J. Li, "Simultaneous wireless information and power transfer (SWIPT): Recent advances and future challenges," *IEEE Commun. Surveys Tuts.*, vol. 20, no. 1, pp. 264–302, 1st Quart., 2018.

[9] L. Liu, R. Zhang, and K.-C. Chua, "Multi-antenna wireless powered communication with energy beamforming," *IEEE Trans. Commun.*, vol. 62, no. 12, pp. 4349–4361, Dec. 2014.

[10] G. Yang, C. K. Ho, R. Zhang, and Y. L. Guan, "Throughput optimization for massive MIMO systems powered by wireless energy transfer," *IEEE J. Sel. Areas Commun.*, vol. 33, no. 8, pp. 1640–1650, Aug. 2015.

[11] H. Lee, K.-J. Lee, H. Kim, B. Clerckx, and I. Lee, "Resource allocation techniques for wireless powered communication networks with energy storage constraint," *IEEE Trans. Wireless Commun.*, vol. 15, no. 4, pp. 2619–2628, Apr. 2016.

[12] D. Hwang, D. I. Kim, and T.-J. Lee, "Throughput maximization for multiuser MIMO wireless powered communication networks," *IEEE Trans. Veh. Technol.*, vol. 65, no. 7, pp. 5743–5748, Jul. 2016.

[13] H. Lee, K.-J. Lee, H.-B. Kong, and I. Lee, "Sum-rate maximization for multiuser MIMO wireless powered communication networks," *IEEE Trans. Veh. Technol.*, vol. 65, no. 11, pp. 9420–9424, Nov. 2016.

[14] T. P. Do and Y. H. Kim, "Resource allocation for a full-duplex wireless-powered communication network with imperfect self-interference cancelation," *IEEE Commun. Lett.*, vol. 20, no. 12, pp. 2482–2485, Dec. 2016.

[15] K. Liang, L. Zhao, K. Yang, and X. Chu, "Online power and time allocation in MIMO uplink transmissions powered by RF wireless energy transfer," *IEEE Trans. Veh. Technol.*, vol. 66, no. 8, pp. 6819–6830, Aug. 2017.

[16] W. Shin, M. Vaezi, J. Lee, and H. V. Poor, "Cooperative wireless powered communication networks with interference harvesting," *IEEE Trans. Veh. Technol.*, vol. 67, no. 4, pp. 3701–3705, Apr. 2018.

[17] J. Choi, C. Song, and J. Joung, "Wireless powered information transfer based on zero-forcing for multiuser MIMO systems," *IEEE Trans. Veh. Technol.*, vol. 67, no. 9, pp. 8561–8570, Sep. 2018.
[18] Z. Wen, S. Wang, C. Fan, and W. Xiang, "Joint transceiver and power splitter design over two-way relaying channel with lattice codes and energy harvesting," *IEEE Commun. Lett.*, vol. 18, no. 11, pp. 2039–2042, Nov. 2014.
[19] Z. Fang, X. Yuan, and X. Wang, "Distributed energy beamforming for simultaneous wireless information and power transfer in the two-way relay channel," *IEEE Signal Process. Lett.*, vol. 22, no. 6, pp. 656–660, Jun. 2015.
[20] Y. Gu and S. Aïssa, "RF-based energy harvesting in decode-and-forward relaying systems: Ergodic and outage capacities," *IEEE Trans. Wireless Commun.*, vol. 14, no. 11, pp. 6425–6434, Nov. 2015.
[21] Y. Liu, L. Wang, M. Elkashlan, T. Q. Duong, and A. Nallanathan, "Two-way relay networks with wireless power transfer: Design and performance analysis," *IET Commun.*, vol. 10, no. 14, pp. 1810–1819, Sep. 2016.
[22] A. Salem and K. A. Hamdi, "Wireless power transfer in multi-pair two-way AF relaying networks," *IEEE Trans. Commun.*, vol. 64, no. 11, pp. 4578–4591, Nov. 2016.
[23] S. Wang, M. Xia, and Y.-C. Wu, "Multipair two-way relay network with harvest-then-transmit users: Resolving pairwise uplink-downlink coupling," *IEEE J. Sel. Topics Signal Process.*, vol. 10, no. 8, pp. 1506–1521, Dec. 2016.
[24] G. Chen, P. Xiao, J. R. Kelly, B. Li, and R. Tafazolli, "Full-duplex wireless-powered relay in two way cooperative networks," *IEEE Access*, vol. 5, pp. 1548–1558, 2017.
[25] T. P. Do, I. Song, and Y. H. Kim, "Simultaneous wireless transfer of power and information in a decode-and-forward two-way relaying network," *IEEE Trans. Wireless Commun.*, vol. 16, no. 3, pp. 1579–1592, Mar. 2017.
[26] N. T. P. Van, S. F. Hasan, X. Gui, S. Mukhopadhyay, and H. Tran, "Three-step two-way decode and forward relay with energy harvesting," *IEEE Commun. Lett.*, vol. 21, no. 4, pp. 857–860, Apr. 2017.
[27] W. Wang, R. Wang, H. Mehrpouyan, N. Zhao, and G. Zhang, "Beamforming for simultaneous wireless information and power transfer in two-way relay channels," *IEEE Access*, vol. 5, pp. 9235–9250, 2017.
[28] J. Rostampoor, S. M. Razavizadeh, and I. Lee, "Energy efficient precoding design for SWIPT in MIMO two-way relay networks," *IEEE Trans. Veh. Technol.*, vol. 66, no. 9, pp. 7888–7896, Sep. 2017.
[29] X. Wang, J. Liu, and C. Zhai, "Wireless power transfer-based multi-pair two-way relaying with massive antennas," *IEEE Trans. Wireless Commun.*, vol. 16, no. 11, pp. 7672–7684, Nov. 2017.
[30] M. Tao and R. Wang, "Linear precoding for multi-pair two-way MIMO relay systems with max-min fairness," *IEEE Trans. Signal Process.*, vol. 60, no. 10, pp. 5361–5370, Oct. 2012.
[31] K. Zu, R. C. de Lamare, and M. Haardt, "Generalized design of low-complexity block diagonalization type precoding algorithms for multiuser MIMO systems," *IEEE Trans. Commun.*, vol. 61, no. 10, pp. 4232–4242, Oct. 2013.
[32] N. D. Sidiropoulos, T. N. Davidson, and Z.-Q. Luo, "Transmit beamforming for physical-layer multicasting," *IEEE Trans. Signal Process.*, vol. 54, no. 6, pp. 2239–2251, Jun. 2006.
[33] Le-N. Tran, M. F. Hanif, and M. Juntti, "A conic quadratic programming approach to physical layer multicasting for large-scale antenna arrays," *IEEE Signal Process. Lett.*, vol. 21, no. 1, pp. 114–117, Jan. 2014.
[34] J. Choi, "Iterative methods for physical-layer multicast beamforming," *IEEE Trans. Wireless Commun.*, vol. 14, no. 9, pp. 5185–5196, Sep. 2015.
[35] J. Choi, "Minimum power multicast beamforming with superposition coding for multiresolution broadcast and application to NOMA systems," *IEEE Trans. Commun.*, vol. 63, no. 3, pp. 791–800, Mar. 2015.
[36] S. X. Wu, A. M.-C. So, J. Pan, and W.-K. Ma, "Semidefinite relaxation and approximation analysis of a beamformed alamouti scheme for relay beamforming networks," *IEEE Trans. Signal Process.*, vol. 65, no. 9, pp. 2428–2443, May 2017.
[37] C.-Y. Wu, W.-J. Huang, and W.-H. Chung, "Robust update algorithms for zero-forcing detection in uplink large-scale MIMO systems," *IEEE Commun. Lett.*, vol. 22, no. 2, pp. 424–427, Feb. 2018.
[38] S. Boyd and L. Vandenberghe, *Convex Optimization*. Cambridge, U.K.: Cambridge Univ. Press, 2004, pp. 133–134.
[39] M. Grant and S. Boyd. (Aug. 2012). *CVX: MATLAB Software for Disciplined Convex Programming*. [Online]. Available: http://cvxr.com/cvx

GERARDO SACARELO received the B.S.E. degree in electronics and telecommunications engineering from Escuela Superior Politécnica del Litoral, Ecuador, in 2014. He is currently pursuing the M.S. and Ph.D. degrees in electronic engineering with Kyung Hee University, South Korea. His research interests include cooperation communication, massive MIMO, and wireless powered communication with energy harvesting.

IICKHO SONG received the B.S.E. *(magna cum laude)* and M.S.E. degrees in electronics engineering from Seoul National University, Seoul, South Korea, in 1982 and 1984, respectively, and the M.S.E. and Ph.D. degrees in electrical engineering from the University of Pennsylvania, Philadelphia, PA, USA, in 1985 and 1987, respectively. He was a Member of the Technical Staff at Bell Communications Research, in 1987. In 1988, he joined the School of Electrical Engineering, Korea Advanced Institute of Science and Technology, Daejeon, South Korea, where he is currently a Professor. He has co-authored a few books including *Advanced Theory of Signal Detection* (Springer, 2002) and *Random Variables and Stochastic Processes* (Korean: Freedom Academy, 2014), and has published papers on signal detection and mobile communications.

Dr. Song is a Fellow of the Korean Academy of Science and Technology (KAST) and IET, and a member of the Acoustical Society of Korea (ASK), the Institute of Electronics Engineers of Korea (IEEK), the Korean Institute of Communications and Information Sciences (KICS), and the Korea Institute of Information, Electronics, and Communication Technology. He has received several awards including the Young Scientists Award (KAST, 2000), the Achievement Award (IET, 2006), and the Hae Dong Information and Communications Academic Award (KICS, 2006). He has served as the Treasurer for the IEEE Korea Section, as an Editor for the *Journal of the ASK*, *Journal of the IEEK*, the *Journal of the KICS*, and the *Journal of Communications and Networks (JCN)*, and as a Division Editor of the *JCN*.

YUN HEE KIM (S'97–M'00–SM'05) received the B.S.E. *(summa cum laude)*, M.S.E., and Ph.D. degrees in electrical engineering from the Korea Advanced Institute of Science and Technology, Daejeon, South Korea, in 1995, 1997, and 2000, respectively. From 2000 to 2004, she was with the Electronics and Telecommunications Research Institute, Daejeon, South Korea, as a Senior Member of Research Staff. In 2004, she joined the Department of Electronic Engineering, Kyung Hee University, Yongin, South Korea, where she is currently a Professor. In 2000 and 2011, she was with the Department of Electrical and Computer Engineering, University of California at San Diego, La Jolla, CA, USA, as a Visiting Researcher. Her research interests include communication theory, statistical signal processing, and wireless communications.